Influence of atmospheric scintillations on image centroid

V.V. Voitsekhovich, V.G. Orlov, and L.J. Sanchez

Institute of Astronomy, Mexico City, Mexico

Received October 30, 2001

The effect of atmospheric scintillations on an image centroid is investigated by means of computer simulations. The simulations were performed for the case of weak turbulence for both varying and constant C_n^2 (vertical and horizontal radiation propagation). It is shown that, under weak-turbulence conditions, the magnitude of the effect does not exceed 15%. However, because it grows up with the increasing turbulence, a quite strong effect of scintillations on the image centroid under the strong-turbulence conditions can be expected. A comparison of the results for vertical and horizontal propagation shows that there is no strong dependence of the effect magnitude on the structure of the C_n^2 profile. Probably, it is mainly determined by two parameters: integral turbulence (Fried parameter) and scintillation level (log-amplitude variance).

Introduction

Measurements of an image centroid are often used in Hartmann-type wavefront sensors to reconstruct the phase distorted by atmospheric turbulence.[1–7] This approach is used both in basic research of atmospheric turbulence and for practical needs (as, for example, in adaptive optics of the atmosphere), as well as in various applications, because it gives a direct and simple relation between measurements and the phase gradient. In this approach, it is assumed that the phase gradient averaged over the subaperture of the Hartmann mask is proportional to the corresponding shift of the image centroid. However, this simple relation is valid only when the effect of amplitude scintillations is ignored. According to the commonly accepted idea,[8] under the conditions of weak turbulence the effect of amplitude scintillations on the image centroid is negligibly small, but this idea has been never checked by computations.

In this paper, we calculate the magnitude of the effect under study by means of the recently proposed method of random wave vectors,[9,10] which allows the simulation of amplitude and phase realizations with desired and mutual statistics.

1. Determination of the error caused by scintillations

Let the wave $\psi(\rho)$ pass through a thin lens with the diameter d and the focal length f. The centroid ρ_c of the image formed by this wave in the focal plane of the lens can be represented as

$$\rho_c = \{x_c, y_c\} = -\frac{f}{k}\,\frac{\int\limits_{G_d} d^2\rho \, \exp[2\chi(\rho)]\,\nabla S(\rho)}{\int\limits_{G_d} d^2\rho \, \exp[2\chi(\rho)]}, \qquad (1)$$

where x_c and y_c are the Cartesian coordinates of the image centroid; $\chi(\rho)$ and $S(\rho)$ are, respectively, the log-amplitude and phase of the wave ψ; k is the wavenumber; G_d means an integration over the lens aperture.

However, in experiments connected with reconstruction of the phase from the image centroid measurements (for example, using Hartmann-type wavefront sensors), the effect of amplitude scintillations on the image centroid is always assumed negligibly small. Mathematically, this assumption can be written as

$$\rho'_c = \{x'_c, y'_c\} = -\frac{f}{k\Sigma}\int\limits_{G_d} d^2\rho\, \nabla S(\rho), \qquad (2)$$

where Σ is the lens area.

Since ρ_c and ρ'_c are random in the problems connected with radiation propagation through the turbulent atmosphere, the relative error σ of image centroid measurements due to amplitude scintillations can be represented as:

$$\sigma = \frac{1}{2}\left[\frac{\sqrt{\langle (x_c - x'_c)^2\rangle}}{\sqrt{\langle x_c^2\rangle}} + \frac{\sqrt{\langle (y_c - y'_c)^2\rangle}}{\sqrt{\langle y_c^2\rangle}}\right]. \qquad (3)$$

From the physical point of view, σ shows how large is the relative contribution of scintillations to the shift of the image centroid. In this paper, this value is calculated by means of numerical simulation depending on turbulence conditions and the lens size.

2. Method of numerical simulation

In this paper, we restrict our consideration to propagation of the initially plane wave through the weakly turbulent atmosphere. In this case, we can use the method of random wave vectors (RWV), which allows a simulation of phase and log-amplitude

0235-6880/02/08 615-04 $02.00

realizations with desired and mutual statistics. Below we give only brief description of the RWV method, because it was considered in detail in Ref. 9.

Realizations of the phase $S(\rho)$ and log-amplitude $\chi(\rho)$ on the aperture are simulated as follows:

$$S(\rho) = \sum_{m=1}^{M} F(p_m) \cos(\mathbf{p}_m \cdot \rho + \varphi_m);$$
$$\chi(\rho) = \sum_{m=1}^{M} G(p_m) \cos(\mathbf{p}_m \cdot \rho + \varphi_m + \psi_m), \qquad (4)$$

where ρ is the two-dimensional radius vector in the aperture plane; M is the number of harmonics used for simulation; $\mathbf{p}_m$ is the two-dimensional random wave vector; p_m is the magnitude of the vector $\mathbf{p}_m$.

The following statistical restrictions are imposed on the parameters in Eqs. (4):

1) The magnitude p_m and direction θ_m of the vector $\mathbf{p}_m$, as well as the parameters φ_m and ψ_m are supposed statistically independent.

2) The values of θ_m and φ_m are distributed uniformly in the interval $[-\pi, \pi]$.

If these conditions are fulfilled, Eqs. (4) allow a direct physical interpretation. Statistical independence on φ_m and the uniform distribution of this parameter in the interval $[-\pi, \pi]$ reduce the problem to consideration of only homogeneous processes. Then isotropic processes are selected from the class of homogenous processes by imposing a random uniform distribution on the interval $[-\pi, \pi]$ for the orientation θ_m of the vector $\mathbf{p}_m$. Thus, with these two restrictions, the parameters S and χ are simulated by isotropic random functions in accordance with the existing theory of atmospheric turbulence.

Then let us select the joint probability density function of the parameters $\mathbf{p}_m$, $F(\mathbf{p}_m)$, $G(\mathbf{p}_m)$, φ_m, and ψ_m in such a way that the model spectra W_S^{mod}, W_χ^{mod}, and $W_{S\chi}^{\text{mod}}$ coincide with the corresponding theoretical spectra W_S, W_χ, and $W_{S\chi}$.

Under the above conditions, the parameters of Eqs. (4) can be expressed through theoretical spectra as follows (for detailed derivation see Ref. 9).

The amplitudes F and G:

$$F(p) = \sqrt{\frac{W_S(p)}{\pi M \Omega(p)}}\ ;\ G(k) = \sqrt{\frac{W_\chi(p)}{\pi M \Omega(p)}}\ . \qquad (5)$$

The probability density function (PDF)

$$\Omega(p) = 1/[2\pi p^2 \log(K_2/K_1)], \qquad (6)$$

where $[K_1, K_2]$ is the interval, in which the values of p are generated.

The joint PDF $\eta(\psi, p)$ of the parameters ψ and p is

$$\eta(\psi, p) = \frac{1}{2\sqrt{\pi\alpha(p)}} \exp\left[-\frac{\psi^2}{4\alpha(p)}\right];$$

$$\alpha(p) = \log\sqrt{\frac{W_S(p)\ W_\chi(p)}{W_{S\chi}(p)}}\ . \qquad (7)$$

Under the conditions of weak turbulence, the theoretical spectra can be obtained from solution of the Rytov parabolic equation as[11]

$$W_S(p) = 0.651\ \Phi_n(p) \int \mathrm{d}z\ C_n^2(z) \left[1 + \cos\left(\frac{z}{k} p^2\right)\right],$$
$$W_\chi(p) = 0.651\ \Phi_n(p) \int \mathrm{d}z\ C_n^2(z) \left[1 - \cos\left(\frac{z}{k} p^2\right)\right],$$
$$W_{S\chi}(p) = 0.651\ \Phi_n(p) \int \mathrm{d}z\ C_n^2(z) \sin\left(\frac{z}{k} p^2\right), \qquad (8)$$

where Φ_n is the spectrum of the refractive index; $C_n^2(z)$ is the profile of the refractive index structure parameter, and the integrals are taken over the radiation propagation path.

The step-by-step description of the simulation procedure can be found in Ref. 9.

3. Results of simulation

Using Eqs. (1)–(3) and simulation by the RWV method, we can estimate the relative error σ given by Eq. (3). The simulation was carried out for the case of Kolmogorov turbulence $\Phi_n(p) = p^{-11/3}$. The following parameters were taken as the main parameters of simulation: limit frequencies $K_1 = 10^{-3}$ m^{-1} and $K_2 = 10^3$ m^{-1}, as well as the number of harmonics $M = 100$. The limit frequencies were taken after a series of preliminary numerical experiments, which showed that further decrease of K_1 and increase of K_2 almost do not change final results. The number of harmonics was chosen in a similar way. The number of realizations used for statistical averaging in Eq. (3) was taken equal to 1000. The simulation was carried out for two cases of radiation propagation that are of interest from the practical point of view: varying C_n^2 (vertical propagation) and constant C_n^2 (horizontal propagation).

For the calculation with varying C_n^2, we used the Hufnagel model[12] for $C_n^2(z)$ in the following form:

$$C_n^2(z) = C_0\ r_0^{-5/3} \times$$
$$\times\ k^{-2}\left[\left(\frac{z}{z_0}\right)^{10} \exp\left(-\frac{z}{z_1}\right) + \exp\left(-\frac{z}{z_2}\right)\right], \qquad (10)$$

where r_0 is the Fried parameter; k is the wavenumber; $C_0 = 1.027 \cdot 10^{-3}$ m^{-3}, $z_0 = 4.632 \cdot 10^3$ m, $z_1 = 10^3$ m, and $z_2 = 1.5 \cdot 10^3$ m.

The equations for the spectra W_S, W_χ, and $W_{S\chi}$ corresponding to the considered model can be found in Ref. 9. The results of simulation are shown in Fig. 1*a* as a dependence of the relative error on the ratio of the lens diameter d to the Fried parameter r_0 for some values of the wavelength λ, the Fried parameter r_0, and the standard log-amplitude deviation σ_χ.

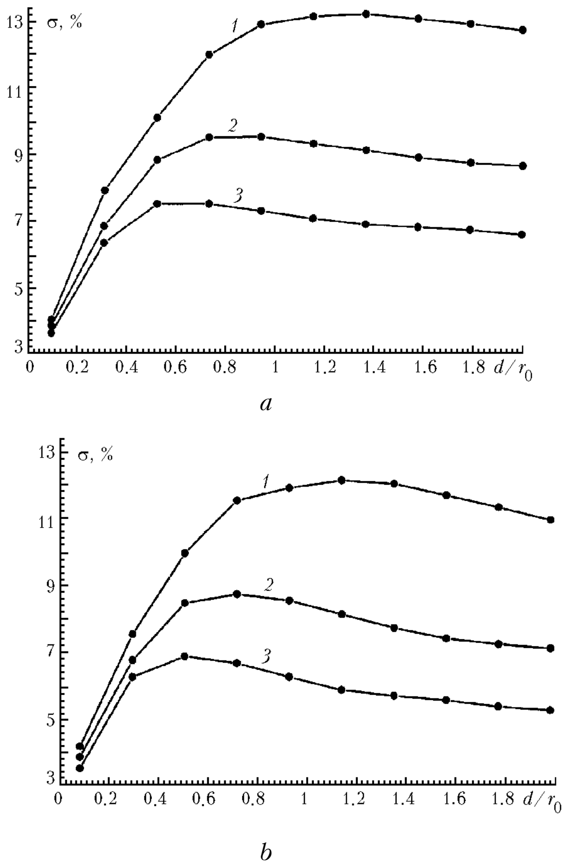

Fig. 1. Relative error σ as a function of the ratio of the lens diameter d to the Fried parameter r_0: vertical radiation propagation (Hufnagel model of the C_n^2 profile) (*a*) and horizontal radiation propagation (*b*); $r_0 = 0.1$ m, $\sigma_\chi = 0.3$ (*1*); $r_0 = 0.15$ m, $\sigma_\chi = 0.21$ (*2*); $r_0 = 0.2$ m, $\sigma_\chi = 0.16$ (*3*); $\lambda = 0.55$ μm.

In the case of horizontal radiation propagation, $C_n^2(z)$ is constant, that is, $C_n^2(z) = C_n^2$. The theoretical spectra can be expressed as follows:

$$W_S(p) = 1.544\, r_0^{-5/3}\, p^{-11/3}\left[1 + \frac{k}{p^2L}\sin\left(\frac{p^2L}{k}\right)\right],$$

$$W_\chi(p) = 1.544\, r_0^{-5/3}\, p^{-11/3}\left[1 - \frac{k}{p^2L}\sin\left(\frac{p^2L}{k}\right)\right], \quad (11)$$

$$W_{S\chi}(p) = 1.544\, r_0^{-5/3}\, p^{-11/3}\frac{k}{p^2L}\left[1 - \cos\left(\frac{p^2L}{k}\right)\right],$$

where L is the radiation path length and $r_0 = 1.68(k^2\, C_n^2\, L)^{-3/5}$.

The results of simulation for the horizontal radiation propagation are shown in Fig. 1*b*. As in the previous case, the relative error is shown as a function of the ratio of the lens diameter to the Fried parameter. For comparison, the path length is taken so that the value of σ_χ is the same as in the previous case.

As can be seen from Fig. 1, the error first increases up to some maximum and then gradually approaches a certain asymptotic value. This behavior can be explained in the following way. As can be seen from Eqs. (1)–(3), this problem involves three different scales: the correlation length of the amplitude, the mutual correlation length of the phase gradient and amplitude, and the correlation length of the phase gradient.

In the initial part, when the aperture size is small as compared to the correlation length of amplitude scintillations, the main contribution to the error is due to the linear components of the amplitude and phase gradient, which provide for the almost linear increase of the error. Then, as the aperture size increases and becomes larger than the correlation length of the amplitude, but still remains small as compared to the mutual correlation length of the phase gradient and amplitude, the nonlinear terms begin to contribute considerably to the error. In this part, the error increases more slowly and in the nonlinear way, when the aperture size becomes comparable with the mutual correlation length of the amplitude and phase gradient. Finally, when the aperture size becomes larger than the mutual correlation length of the amplitude and phase gradient, the main contribution to the error is introduced by such aperture zones, which have the size comparable with the mutual correlation length of the amplitude and phase gradient. In this part, we can see that the error slowly approaches the asymptotic value.

From comparison of Figs. 1*a* and *b*, we can conclude that the magnitudes of the studied effect only slightly differ in the two sensing schemes under consideration. This means that the effect depends insignificantly on the detailed structure of the C_n^2 profile, and it is determined most likely by the two integral parameters of the C_n^2 profile: the integral turbulence (Fried parameter) and the scintillation level (log-amplitude variance).

Conclusion

The effect of amplitude scintillations on image centroid measurements has been assessed. The results obtained show that the magnitude of this effect does not exceed 15% under the conditions of weak turbulence. However, this effect grows up with the increase of turbulence. Therefore, amplitude scintillations can be expected to have a quite strong effect on the image centroid under the conditions of strong turbulence, and, starting from some turbulence level, the reconstruction of the phase from centroid measurements can become impossible.

The magnitude of the studied effect was assessed for two schemes of radiation propagation: constant C_n^2

(horizontal propagation) and C_n^2 varying along the path (vertical propagation). Comparison of the results shows that the difference between these two schemes is small. This means that the effect depends largely on the integral parameters of the C_n^2 profile: Fried parameter and log-amplitude variance, rather than on the detailed structure of the profile.

References

1. V.V. Voitsekhovich, V.B. Gubin, and A.V. Mikulich, Opt. Atm. **1**, No. 5, 66–70 (1988).
2. F. Rigaut, G. Rousset, P. Kern, J.C. Fontanella, J.P. Gaffard, and F. Merkle, Astron. and Astrophys. **250**, 280–290 (1991).
3. W. Jiang, H. Li, C. Liu, X. Wu, S. Huang, H. Xian, Z. Rong, C. Wang, M. Li, N. Ling, and C. Guan, in: *Proc. ICO-16 Satellite Conf. on Active and Adaptive Optics*, ed. by F. Merkle (ICO 16 Secretariat, Garching, Germany, 1993), pp. 127–135.
4. H. Li, H. Xian, and W. Jiang, in: *Proc. ICO-16 Satellite Conf. on Active and Adaptive Optics*, ed. by F. Merkle (ICO 16 Secretariat, Garching, Germany, 1993), pp. 21–25.
5. D. Colucci, M. Lloyd-Hart, D. Wittman, R. Angel, A. Ghez, and B. McLeod, Publ. Astron. Soc. Pacif. **106**, 1104–1110 (1994).
6. F. Rigaut, B.L. Ellerbroek, and M.J. Northcott, Appl. Opt. **36**, 2856–2868 (1997).
7. V.V. Voitsekhovich, J. Opt. Soc. Am. A **8**, 1749–1757 (1996).
8. F. Roddier, Progr. in Optics **19**, 281–376 (1981).
9. D. Kouznetsov, V.V. Voitsekhovich, and R. Ortega-Martinez, Appl. Opt. **36**, 464–469 (1997).
10. V.V. Voitsekhovich, D. Kouznetsov, V.G. Orlov, and S. Cuevas, Appl. Opt. **38**, 3985–3992 (1999).
11. V.I. Tatarskii, *The Effects of the Turbulent Atmosphere on Wave Propagation*, National Science Foundation Report TT-68-50464 (1968).
12. R.E. Hufnagel, in: *Optical Propagation through Turbulence*, OSA Technical Digest Series (OSA, Washington, D.C., 1974), pp. WA1-1–WA1-4.